Electrokinetic extraction and recovery of biosurfactants using rhamnolipids as a model biosurfactant

Brian Gidudu * *and Evans M. Nkhalambayausi Chirwa*

Water Utilisation and Environmental Engineering Division, Department of Chemical Engineering, University of Pretoria, Pretoria 0002, South Africa

*****Correspondence: briangid38@gmail.com**;** Tel: +27 12 420 5894

Abstract

An electrokinetic system was evaluated for the possibility of extracting and recovering of biosurfactants in this study. This was done in a uniquely built electrokinetic reactor with two electrode chambers and a medium chamber separated by a membrane. The voltage applied was varied from 30 V, 20 V to 10 V to evaluate the effect of the voltage used on the process. The results obtained revealed that the electrokinetic system can efficiently extract and recover biosurfactants from the culture broth. The biosurfactants electromigrated towards the anode compartment where they aggregated into fine solids to allow recovery. The highest extraction and recovery of 69.33 ± 3.67 % was achieved under the highest voltage of 30 V followed by 20 V with 9.63 ± 0.4 % and 10 V with 4.98 ± 0.46 %. The biosurfactants extracted using the electrokinetic system had fewer impurities than the extract recovered by acid precipitation. However, the functional groups and retardation factors of all the extracts recovered by acid precipitation and the electrokinetic system were the same.

Keywords: Electrokinetic; Biosurfactants; Electroosmosis; Rhamnolipids

1. Introduction

In the last few decades, biosurfactants have received a lot of attention as prospective substitutes for synthetic surfactants [1]. Biosurfactants are high or low molecular surface-active compounds produced or excreted by microorganisms [2]. Biosurfactants have greater biodegradability, bioavailability, ecological acceptability, biocompatibility, higher selectivity, and lower toxicity as compared to synthetic surfactants [1, 3]. Biosurfactants are now utilised in various applications such as in crude oil drilling lubricants, enhanced oil recovery, biosurfactant-aided bioremediation of hydrophobic pollutants, and formulations in the food, pharmaceutical and cosmetics industry, among others [4, 5]. Some of the widely used biosurfactants are rhamnolipids which are glycolipid biosurfactants produced mainly by *Pseudomonas aeruginosa* [5]. With a chain length ranging from eight to fourteen carbon molecules, rhamnolipids usually contain three hydroxy fatty acid molecules and two rhamnose molecules [6].

The production process of biosurfactants requires cost-effective methods for both upstream and downstream operations to allow its wide use as a replacement for synthetic surfactants [6]. Optimisation of the production process to improve biosurfactant yields and the use of cheaper substrates have been attempted to improve the upstream manufacturing process that mainly involves fermentation operations [6-8]. However, very few efforts have been made towards the

improvement of the downstream processing of biosurfactants much as it is claimed that it constitutes 60-80% of the general production costs [6-8]. The downstream process mainly involves the separation of cells, isolation/recovery of the crude product and concentration/purification of the product [7]. The major challenge experienced during downstream processing is the complexity of the broth, product with multiple congeners and low biosurfactant concentration in the broth [7]. In the past, several conventional methods such as acid precipitation, adsorption on wood-activated carbon, solvent extraction (using Methyl tertiary-butyl ether), organic solvent extraction, centrifugation, ammonium sulfate extraction, foam fractionation, ion-exchange chromatography, membrane ultrafiltration, and adsorption on polystyrene resins have been used [3, 7, 8]. But these purification methodologies do not enable continuity in the production process, are inefficient in ensuring purity and must be used in series as a multi-step strategy which increases the overall costs and complexities of the production process [3, 6]; this is beside the fact that most of the solvents that are used in these processes such as chloroform, methanol and acetone are toxic and adversely affect the environment [8].

In this study, we focused on the downstream production stage by developing a new cleaner and sustainable method of biosurfactant extraction and recovery that can offer continuity of the process from upstream to downstream while eliminating the complexities involved in all the conventional methods that have

been used in the past. To do this, the possibility of extracting and recovering biosurfactants using an electrokinetic/electrochemical system was studied. The use of the ion transport phenomena has been used in several applications such as drug delivery, separation and mobility of nano molecules and nanopore based biosensing [9], but has not been tested for the extraction of biosurfactants yet it can offer efficient, sustainable and cleaner alternatives for the extraction and recovery of the greatly needed biosurfactants [10]. The electrokinetic system is composed of the anode and cathode as electrodes placed on either side of the porous medium [11]. The system utilises current applied across the two electrodes to create an electric field that facilitates the movement of the liquid phase by electroosmosis (electroosmotic flow), charged colloidal particles by electrophoresis and charged ions by electromigration [11]. The movement of the liquid phase by electroosmosis happens when the surface of the vessel in contact with the electrolyte acquires a net surface charge by disassociation or association of the surface functional groups or the absorption of ions on the surface of the vessel [9]. Depending on the dominant charge, the surface attracts preferred counterions and repels ions of a similar charge to create an electric double layer [12]. Then excess counterions with the diffuse layer of the electrical double layer experience a net non-zero electromotive force under the influence of an electric field [9]. Due to the solvate nature of the ions, they drag water molecules with them as they move to electrodes of opposite charge leading to the flow of the liquid phase [9, 13]. On the other hand, the movement of colloidal particles under

the influence of an electric field is based on the differences in the velocities of the particles which is the product of the electric field strength and the particle mobility [14]. Particle mobility is determined by the size of the particle, shape of the particle, the charge of the particle and the temperature during separation [14]. In this study, the ability of the electrokinetic system to recover biosurfactants was evaluated based on the fact that biosurfactants like synthetic surfactants can either be anionic, non-ionic, cationic or zwitterionic with their charge dependent on the carboxyl groups with a pKa less than the pH of the solution in which they are made [15, 16]. It is from this that the electrokinetic system was evaluated because if biosurfactants are charged, it means they could be electromigrated to either the anode or cathode, depending on the charge. Electrochemical methods are generally more advantageous because they hardly require supplementary chemicals, they hardly produce waste and they have an insignificant footprint [17]. Furthermore, the merger of electrochemical methods with cleaner energy sources permits a sustainable panacea for the future [10].

2. Methods and materials

2.1 Microbiological culture, growth medium and biosurfactant production

The production of the biosurfactant was done using a great biosurfactant producing strain (*Pseudomonas aeruginosa*) already identified in our previous studies [18]. The growth medium was composed of 2 mL of trace elements and 4.43 g KH_2PO_4; 7.59 g $Na_2HPO_4 \times 2H_2O$; 0.4 g $MgSO_4 \times 7H_2O$; 6.0 g $(NH_4)_2SO_4$; 0.4 g $CaCl_2 \times 2H_2O$ dissolved in 1 L of type II distilled water [19]. The solution of trace elements was composed of 0.18 g L^{-1} $ZnSO_4 \times 7H_2O$, 0.10 g L^{-1} $MnSO_4 \times H_2O$, 0.16 g L^{-1} $CuSO_4 \times 5H_2O$, 0.18 g L^{-1} $CoCl_2 \times 6H_2O$ and 16 g L^{-1} $FeCl_3 \times 6H_2O$, 20.1 g L^{-1} EDTA [19]. The mineral salt growth medium (MSM) was always autoclaved at 121 ^oC for 15 min before use.

Biosurfactant production started with the inoculation of a pure strain of *Pseudomonas aeruginosa* in 200 mL of sterile nutrient broth contained in an Erlenmeyer flask. The cells were left to grow for 24 h at 250 rpm, temperature of 35 ^oC, and pH of 7. The cells were then harvested for 10 min at 4 ^oC and 10,000 rpm. For massive production of biosurfactant, the harvested cells were moved to 1000 mL of MSM supplemented with 3 % glycerol (v/v) in 3 L Erlenmeyer flasks. The flasks were incubated for 96 h at 35 ^oC, 250 rpm and pH of 7.

To identify and purify the biosurfactant, the biosurfactant was recovered by acid precipitation using aliquots of 100 mL of the supernatant according to Noparat et al. [20]. This was done by removing the cells from the broth by centrifugation for

20 min at 12000 rpm and 4 ^{o}C. The biosurfactant precipitate was obtained by adding 6 N HCl to adjust the pH to 2. This was followed by centrifugation for 20 min at 12,000 rpm and 4 ^{o}C. The biosurfactant was extracted by adding chloroform and methanol (2:1) to the extract and left in the vacuum for the solvents to evaporate. The residue left after evaporation was dissolved in methanol and filtered through a filter (0.22 mm, Millipore). The crude biosurfactant obtained was purified through a column of silica gel to remove impurities. The crude biosurfactant was eluted through methanol and chloroform in 20:80 v/v, then 65:35 v/v to remove the remaining impurities. The biosurfactant was now ready for analysis.

2.2 Determination of the ionic character of the biosurfactant

The double diffusion technique was used to determine the ionic charge of the purified biosurfactant [21]. A pure compound of 20 mM of sodium dodecyl sulfate was used as the compound of anionic charge, and 50 mM barium chloride was used as the compound of cationic charge. The ionic charge was determined by creating two rows in 1% agar plated on Petri dishes. The wells in one row were filled with the purified biosurfactant, and the wells in the adjascent rows were filled with the cationic and anionic compounds. The ionic nature of the biosurfactant was determined by monitoring the precipitation lines at room temperature for 48 h.

2.3 Identification of the biosurfactant using Ultra-Performance Liquid Chromatography-Mass Spectrometry (UPLC-MS)

The analysis was done using an Ultra-high-performance liquid chromatography-quadrupole time-of-flight mass spectrometer at the LC-MS Synapt Facility of the Department of Biochemistry at the University of Pretoria. The UPLC was calibrated using sodium formate clusters in a mass range of 100–3000 Da in ESI mode and to obtain ions in negative and positive mode. The instrument was configured to collect high energy (ramp: 20–40 V) for structure elucidation and low energy precursor (4 V) product spectra by operating the instrument in MS^E mode. The spectrometry was done by injecting 5 µL of the analyte into a Waters C_{18} BEH 1.7 µm (2.1×100 mm) column together with water and acetonitrile containing 0.1% formic acid. Acetonitrile and water were used as the mobile phase run with a 20 min gradient at a flow rate of 0.4 µL/min. The 20 min gradient of acetonitrile: water started with a run time of 5 min for a volume of 30% v/v followed up with 8 min for 30–100% v/v, 2 min for 100% v/v, 1 min for 100–30% v/v and 4 min for 30% v/v. At a constant flow rate of 5 mL/min, the solution of leucine enkephalin (2 ng µL) was used as the lock mass. The ion modes were obtained at a capillary voltage of 2.8 KV, source temperature of 100 ^oC, cone voltage of 30 V with can gas of 100 L/h, the scan time of 0.5 s, and desolvation temperature of 300 ^oC with desolvation gas of 500 L/h

2.4 Electrokinetic set up.

The electrokinetic reactor was constructed from acrylic glass material to have three equal compartments (90 mm ×100 mm ×150 mm) that would make up the anode compartment, medium compartment, and cathode compartment (**Scheme 1**). Graphite electrodes with 20 mm diameter and 100 mm length were connected to the DC power supply (0-3 RS-IPS 303A, 0-30 V) and positioned in the two electrode compartments to be 105 mm away from each other as per the reactor design. The electrode compartments were filled with deionised water, and electrode-medium compartment interfaces were sealed with a cellulose filtration membrane (Metrohm 627140020, 0.2 μm) to prevent the flow of the cells from the medium compartment but to allow electroosmotic flow (EOF) and movement of the biosurfactant across the compartments. The voltage applied was varied from 30 V to 20 V to 10 V as per the capacity of the DC power supply to evaluate the effect of voltage on the extraction and recovery process of the biosurfactant. The culture broth containing dissolved biosurfactant was introduced in the medium compartment at the beginning of the experiment. Then, temperature, pH, oxidation-reduction potential (ORP), and conductivity were monitored in each of the compartments. Conductivity and temperature were measured using a Thermo Scientific Orion DuraProbe cell. The current and voltage were measured using a digital UT61C multimeter from UNI-T. The ORP and pH were measured using PL-700 Series bench top meters. Electroosmotic flow was determined as the electrolyte volume that moved and accumulated in either of the electrode

compartments [22, 23]. The material recovered after the electrokinetic process in either electrode compartments was then identified.

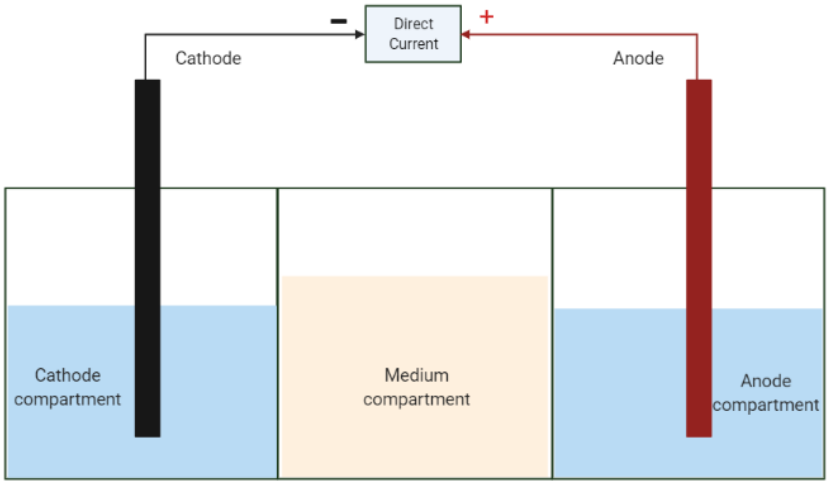

Scheme 1. Schematic view of the electrokinetic system setup

2.5 Evaluation of the purity of the extracts (recovered biosurfactant)

The purity of the extract recovered in the anode compartment was analysed using Energy Dispersive X-Ray Analysis (EDX), Fourier Transform Infrared Spectroscopy (FTIR) and Thin Layer Chromatography (TLC). In TLC, the retardation factors of the extract obtained after acid precipitation were compared to the retardation factors of the extract recovered in the anode compartment after electrokinetic extraction. The functional groups of the extract obtained by acid precipitation were also compared to the functional groups of the extract obtained by the electrokinetic process using the FTIR. These were all done as seen below.

2.2.1 Thin Layer Chromatography.

The biosurfactant extracted by acid precipitation (Acid_Bio) and those extracted by the electrokinetic system at 30 V, 20 V and 10 V (EKS_Bio_30 V, EKS_Bio_20 V and EKS_Bio_10 V) were dissolved in methanol and separated on silica gel plates to assess the differences or similarities in the composition of the recovered extracts. The procedure was done according to Shreve and Makula [24], where the silica gel thin-layer plates were developed in a chamber containing chloroform/methanol/water-concentrated ammonium hydroxide (75:25:2:1, by volume) and visualised by spraying the plates with 75% sulfuric acid followed by heating for 10 min at 100 ^{o}C. The retardation factors of the four spots of different biosurfactant extracts were then determined.

2.2.2 Fourier transform infrared spectroscopy.

The FTIR (Perkin Elmer 1600 was used to elucidate the composition of the purified biosurfactant obtained after acid precipitation by identifying the functional groups of the extract. 5 mg of the purified extract was pulverised with 80 mg of KBr. The fine powder was pressed for 30 s with a load to obtain thin pellets. The scan was performed with a resolution of 2 cm over a wavenumber of 400-4000 cm^{-1} [25].

2.6 Energy Dispersive X-Ray Analysis and Scanning Electron Microscopy

Scanning Electron Microscopy (SEM) and Energy Dispersive X-Ray Analysis (EDX) were done using a Zeiss Gemini Ultra Plus 540 FEG with SEM and EDS detectors at the Laboratory for Microscopy and Microanalysis at the University of Pretoria. The analysis was done for the solid samples of the biosurfactant extract obtained by acid precipitation and those obtained by the electrokinetic recovery process. The SEM was done for samples coated with carbon while EDX was done for samples coated with gold. The structure, morphology and size of the particles were obtained by SEM while the elemental and chemical analysis of the samples was done by EDX.

2.7 ANOVA statistical analysis

The statistical analysis of the data obtained was done by analysis of variance (ANOVA). Turkey's test was run to do a post-doc analysis of the data obtained. The significance in the differences of the means of the independent variables compared were considered significant if $P \leq 0.05$. ANOVA was done to determine the differences between the results obtained by comparing the values of current, conductivity, EOF, temperature and biosurfactant recovery of the three experiments (30 V and 20 V, 30 V and 10 V, 20 V and 10 V).

3. RESULTS AND DISCUSSION

3.1 Identification of the biosurfactant produced by the bacteria using Ultra-Performance Liquid Chromatography-Mass Spectrometry (UPLC-MS)

The biosurfactant purified after acid precipitation recovery was identified before evaluating the electrokinetic extraction method. The chromatographs obtained were analysed using the the MassLynx V4.1 (Waters) software (**Fig. 1**). The LC-MS/MS spectrometry of the biosurfactant revealed the presence of a rhamnolipid biosurfactant with four di-rhamnolipid congeners and seven mono-rhamnolipid congeners (**Table 1**). The seven mono-rhamnolipids produced were composed of four mono-rhamno-mono-lipidic congeners and three mono-rhamno-di-lipidic congeners while the di-rhamnolipids were mainly composed of di-rhamno-di-lipidic congeners. These observations are similar to the reports made when the same strain was used to produce a rhamnolipid biosurfactant in different environmental conditions [26].

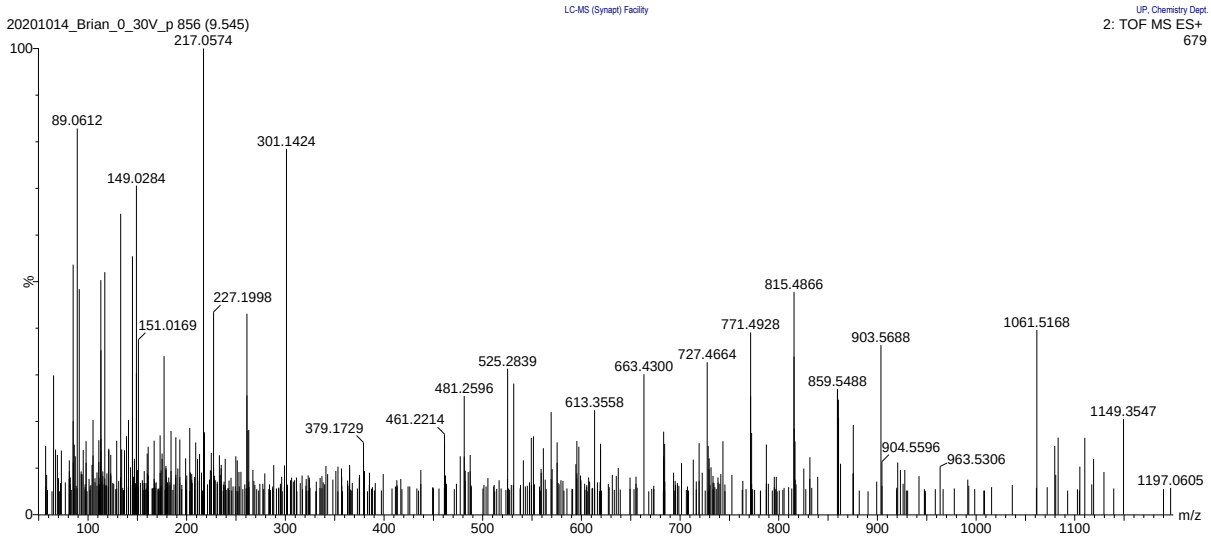

Fig. 1. Mass-Charge spectrum of the biosurfactant obtained by liquid chromatography tandem mass spectrometry

Table 1. Components of the rhamnolipid biosurfactant

[M+H] (m/z)	Rhamnolipid components	Molecular formula	Mass defect (±)
Mono-rhamno-mono-lipidic congeners			
302.158776	Rha-$C_{8:2}$	$C_{14}H_{22}O_7$	-0.0110
334.227676	Rha-C_{10}	$C_{16}H_{30}O_7$	-0.0285
358.22756	Rha-$C_{12:2}$	$C_{18}H_{30}O_7$	-0.0284
386.296976	Rha-$C_{14:2}$	$C_{20}H_{34}O_7$	-0.0666
Mono-rhamno-di-lipidic congeners			
502.6653	Rha-C_{10}-$C_{10:1}$	$C_{26}H_{46}O_9$	-0.3511
518.377276	Rha-C_{10}-C_{10}-CH_3	$C_{27}H_{50}O_9$	-0.0318
532.42746	Rha-C_{10}-C_{12} or Rha-C_{12}-C_{10}	$C_{28}H_{52}O_9$	-0.27954
Di-rhamno-di-lipidic congeners			
650.571776	Rha-Rha-C_{10}-C_{10}	$C_{32}H_{58}O_{13}$	-0.1840

664.465176	Rha-Rha-C_{10}-C_{10}-CH_3	$C_{33}H_{60}O_{13}$	-0.0618
678.488776	Rha-Rha-C_{10}-C_{12} or Rha-Rha-C_{12}-C_{10}	$C_{34}H_{62}O_{13}$	-0.0697
735.5540	Rha-Rha-C_{12}-C_{14} or Rha-Rha-C_{14}-C_{12}	$C_{38}H_{70}O_{13}$	0.03937

3.2 Effect of voltage on current and conductivity

In all the experiments, the current started low in the first 2 h with 30 V at 2.43 ± 0.3 mA, 20 V at 1.585 ± 0.065 and 10 V at 0.625 ± 0.015 mA (**Fig. 2**). The current then gradually increased for the next 4 h in the experiment where 30 V was applied. This was also observed in the experiment where 20 V was used much as the current only increased for 2 h. The current decreased after that to the end of the investigation for both 20 V and 30 V. In the experiment where 10 V was applied, the current remained constant for the first 2 h after that reduction occurred until the end of the experiment. The values of current obtained showed a statistically significant difference when 30 V and 10 V were compared (P = 0.001), but the other comparisons (30 V and 20, 10 V and 20 V) were not statistically significant.

The time course of current is also explained by the conductivity monitored in the system (**Fig. 3**). In the cathode and anode compartments, the initial conductivity of the electrolyte was 0.08 ± 0.047 mS/m. In the cathode compartment, the conductivity increased to 30.65 ± 0.15 mS/m, 15.095 ± 2.7

mS/m, and 2.78 ± 1.28 mS/m for 30 V, 20 V and 10 V respectively within 10 h. In the anode compartment, the conductivity also increased to 24.05 ± 2.95 mS/m, 11.24 ± 1.21 mS/m, and 1.45 ± 0.05 mS/m for 30 V, 20 V and 10 V respectively. The conductivities in the cathode compartment were higher than the conductivities in the anode compartment for each of the voltages applied due to the loss of the electrolyte towards the cathode by electroosmosis. In the medium compartment, the conductivity of the culture broth had an initial conductivity of 42.75 ± 2.55 mS/m but increased to 86.45 ± 0.45 mS/m in 10 h when 20 V was applied. It, however, reduced to 38.55 ± 0.85 mS/m and 34.35 ± 1.95 mS/m when 30 V and 10 V were applied, respectively. In fact, the conductivity in the medium compartment remained constant after 6 h when 10 V was used. The conductivity in the medium compartment was very high when 20 V was applied because of the high accumulation of OH^- and H^+ ions within the medium compartment due to their low drift velocity, which is a function of current/voltage. This was different when 30 V was used, where the conductivity was high at the beginning of the experiment but kept reducing to the end of the experiment since ions were travelling faster to their positively charged electrodes due to the increase in current (resulting from the increase in voltage from 20 V to 30 V) [27]. When 10 V was applied, the conductivity reduced in the first 2 h and remained constant until the end of the experiment. The low conductivity is because of the low energy involved in the electrolysis of water leading to the production of low ion concentrations in the system and, consequently, the low drift velocity picked

up by the produced ions. This shows why the current was high when 30 V was applied but remained very low when 10 V was applied. In the first 6 h, the current was generally high in all the three experiments operated at different voltages because of the disassociation of water into OH^- and H^+ ions as a result of the high electric field intensity applied at the electrodes [27]. The introduction of these ions in the system increased the system's ionic strength, leading to an increase in the current [11, 27]. The conductivity values obtained in the cathode compartment showed a statistically significant difference when 30 V and 10 V were compared (P = 0.001), while all the other comparisons were insignificant. In the medium compartment and anode compartment, the conductivities obtained do not have a statistically significant difference (P = 0.437 and P = 0.454, respectively).

When current flows through a liquid or solid, the electrical energy is converted into thermal energy due to resistive losses by a process also known as Joule heating [28]. The thermal energy generated by the material is proportional to the product of its resistance, the square of its current and the time the current is allowed to flow [29]. In our experiments, this was observed when temperature increased with an increase in voltage/current. As seen in **Fig. 3**, the temperature started at 25.55 ^oC at the beginning of the experiment but continuously increased up to the end of the investigation when 30 V and 20 V was applied, while the temperature remained low in all the compartments when 10 V was used. In the cathode compartment, the current increased to 35.6 ± 0.2 ^oC and 28.75 ^oC for 30

V and 20 V, respectively. In the medium compartment, the temperatures rose to 37.6 ± 1 ºC for 30 V and 28.45 ± 0.65 ºC for 20 V. In the anode compartment; the temperatures increased to 38.15 ± 0.45 ºC for 30 V and 29.75 ± 0.85 ºC for 20 V in 10 h. In the experiment where 10 V was applied, the temperatures remained in the range of 27 ºC to 25.4 ºC in all the electrokinetic system compartments. The temperatures did not increase to the extent of imposing a significant effect on the extraction process. The temperature values obtained in the cathode compartment showed a statistically significant difference when 30 V and 20 V were compared (P = 0.001) while the other comparisons were insignificant. The conductivities obtained in the medium compartment and anode compartment did not have a statistically significant difference (P = 0.437 and P = 0.454, respectively).

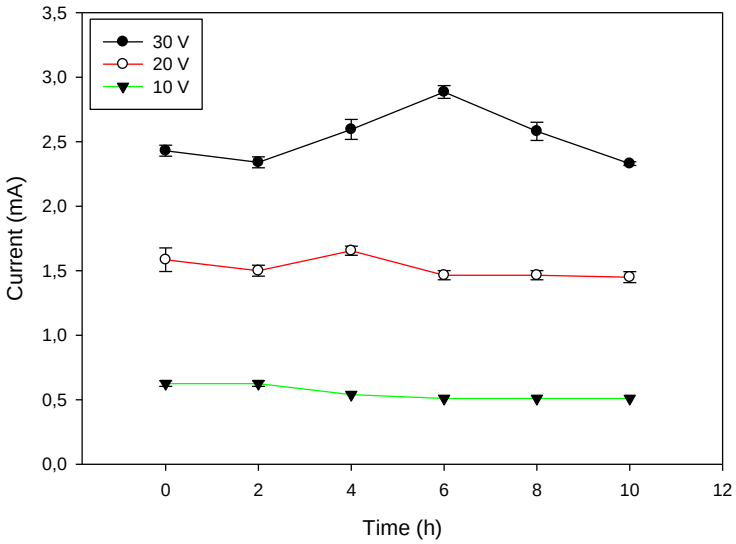

Fig. 2. Time course of current in the electrokinetic system at different voltages of 30 V, 20 V and 10 V.

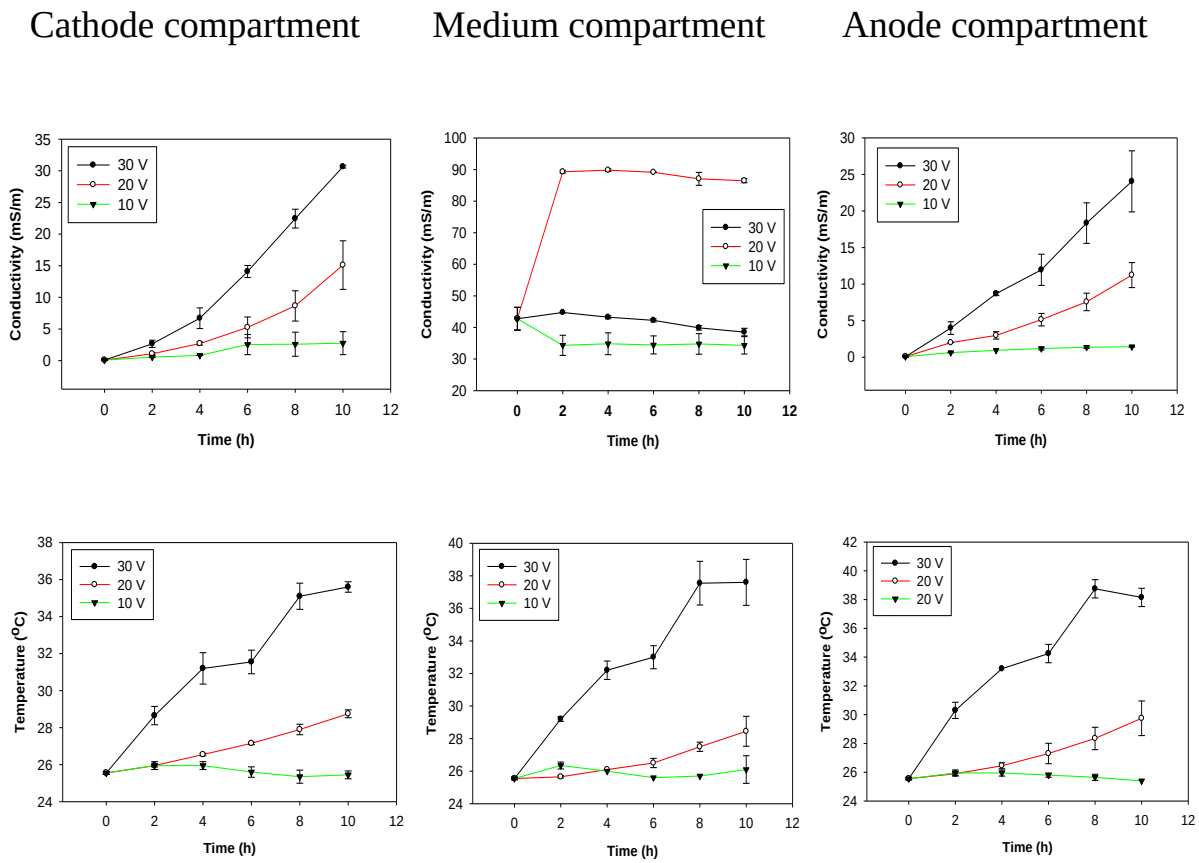

Fig. 3. Time course of conductivity and temperature in the three compartments of the electrokinetic system as a function of different voltages applied. Results are a representation of the mean of three experiments, and errors bars represent the standard deviation.

3.3 Relationship between electroosmosis and voltage (current)

The presence of an electric field in an electrokinetic system creates an electrical double layer at the interface of the electrolyte (liquid phase) and the solid surface of the electrokinetic system that causes the movement of the liquid phase from one compartment to another [30]. The results showing the trends of electroosmosis in terms of electroosmotic flow (EOF) are shown in **Fig. 4**. The flow of the electrolyte (anolyte) from the anode compartment towards the cathode

compartment was observed. The EOF of the anolyte from the anode compartment towards the cathode shows that the media in the medium compartment was predominantly positively charged. Due to the negative nature of the surface of the wall, preferential counterions positive in nature are formed on the surface of the wall. These ions are solvated so drag the water molecules around them as they move due to the influence of the electric field towards the cathode, an electrode of opposite charge [30]. In the experiment where 30 V was applied, the EOF started high at 18000 mm^3 in the first 2 h and generally kept increasing after 4 h until the end of the experiment. At the elapse of 10 h, more than 47250 mm^3 of the electrolyte (anolyte) had moved from the anode compartment towards the cathode compartment under the application of 30 V. When 20 V was used, no EOF was observed for the first 4 h. After 4 h, the EOF was then observed and continuously increased until the end of the experiment with more than 9000 mm^3 of the anolyte lost from the anode compartment towards the cathode. When a voltage of 10 V was applied, EOF was not observed until 8 h elapsed. A volume of 4500 mm^3 of the anolyte was then lost in the next 2 h before the end of the experiment.

Considering Helmholz–Smoluchowski theory represented by the equation below (**Eq. (1))** as cited by other researchers [15, 31] to include the electric field (E_x), electroosmotic flow (EOF), dielectric constant (D), vacuum permittivity ($\mathcal{E}_0$), and fluid viscosity (l), it is revealed that the results obtained in our studies

are not in total agreement with the theory since the EOF was not directly proportional to the voltage (current) applied. The increase in voltage from 10 V to 20 V to 30 V should have led to a corresponding rise in EOF at every increment, but this was not the case. The increase in voltage from 10 V to 20 V led to a 2-fold increase in EOF, but the increase in voltage from 20 V to 30 V led to a 5-fold increase in EOF. The EOF obtained at 20 V was, therefore, lower than it should have been under perfect conditions. The low values of EOF observed when 10 V was applied were because of the low electrolytic current that resulted from the low conductivity of the system, as shown in **Fig. 3**. But when 20 V was applied, the EOF was somewhat affected by the high accumulation of OH^- ions moving from the anode to the medium compartment. This is revealed by high ORP measurements obtained in the medium compartment after 2 h with a profile similar to the ORP profile at the anode (**Fig. 3**). The increase in ionic strength of the medium can affect the magnitude of EOF due to the reduction of the double layer, and that is why the EOF at 20 V was lower than expected [32-34]. The EOF of the electrolyte from the anode compartment towards the cathode compartment improves the extraction and recovery of the biosurfactant in several ways, such as reducing the anolyte (water content) in the biosurfactant recovered in the anode compartment. The reduction in the anolyte also concentrates the biosurfactant in one compartment where it is recovered. This is why the extracts recovered using 30 V were highly turbid as compared to other voltages with highly suspended extracts in the anolyte. The EOF values showed a statistically significant

difference when 30 V and 10 V were compared (P = 0.001), while the other comparisons were insignificant since the differences were not high enough.

$$EOF = \frac{-D\varepsilon_0 Z}{\mu} E_x \quad (1)$$

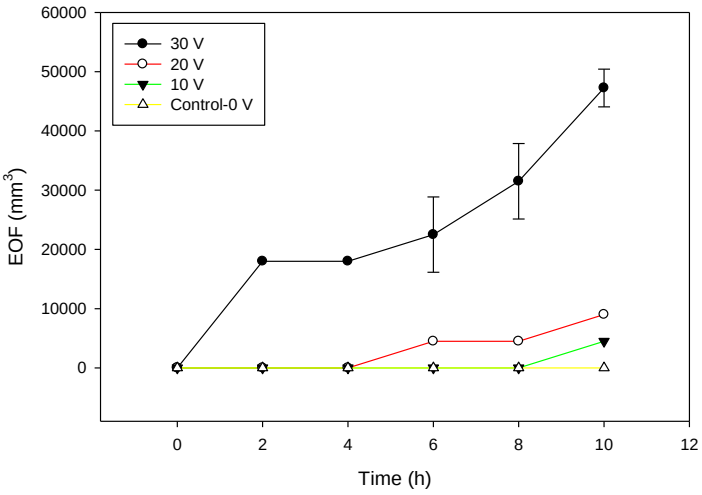

Fig. 4. Electroosmotic flow in the electrokinetic system as a function of different voltages applied. Results are a representation of the mean of three experiments, and errors bars represent the standard deviation.

3.4 The effect of voltage (current) on pH and ORP

The pH and the ORP of the system are mainly dependent on the decomposition of water at the electrodes [19]. The pH in each of the reactor compartments is shown in **Fig. 5**. The pH of the anolyte and catholyte started at 7.895 ± 0.42 in all the experiments. In the medium compartment, the pH of the biosurfactant broth started at 7.56 ± 0.07. When the current was applied, the pH at the cathode continuously increased in all experiments. After 10 h the pH had reached 13.475 ± 0.005 for 30 V, 13.97 ± 0.05 for 20 V and 10.595 for 10 V. In the medium

compartment, the pH was high at the medium-cathode interface and very acidic at the medium-anode compartment interface. The pH in the medium compartment was 6.63 ± 0.05 for 30 V, 7.34 ± 0.04 for 20 V and 7.37 ± 0.015 for 10 V after 10 h. At the anode, the conditions were highly acidic with the pH reaching 1.165 ± 0.05 for 30 V, 2.49 ± 0.03 for 20 V and 4.77 ± 0.46 for 10 V after 10 h. The results show that for the lowest pH conditions to be reached in the anode compartment, the voltage must be high. This explains why the pH was 1.165 ± 0.05 when 30 V was applied compared to 4.77 ± 0.46 when 10 V was applied. As Shu, Liu, Liu, Du and Tao [35] described, the highly alkaline conditions at the cathode are due to the production of OH^- ions because of oxidation reactions. In contrast, the highly acidic conditions at the anode are due to the generation of H^+ ions due to reduction reactions as seen in the equations below (Eqs. (2) and (3)). Due to electromigration, the generation of OH^- ions at the cathode creates an alkaline front at the cathode moving towards the anode and an acidic front at the anode, moving towards the cathode [27]. This creates a pH gradient across the electrokinetic system until H^+ ions meet OH^- ions to create water, with the movement of the H^+ ions (acidic front) almost as twice as fast as the movement of OH^- ions (alkaline front) [27, 35].

To further determine the effect of pH on the system, ORP was monitored as seen in **Fig. 5**. The low ORP indicates oxidising reactions at the cathode, while the high ORP values represent the reduction reactions at the anode. At the

cathode, the ORP reduced from -67.5 ± 2.5 to -415 ± 4 mV, -390.5 ± 4.5 mV, and -249.5 ± 1.5 mV for 30 V, 20 V and 10 V, respectively. At the anode, the ORP increased from -67.5 ± 2.5 to 409.1 ± 5 mV, 366.75 ± 3.05 mV, and 30.1 ± 1.4 mV for 30 V, 20 V and 10 V, respectively. In the medium compartment, the ORP started at 12 mV and increased to 32.2 ± 5.9 for 30 V and 45.8 ± 3.6 for 20 V but reduced to -49.05 for 10 V. The values of pH obtained in the cathode compartment showed a statistically significant difference only when 30 V and 10 V were compared (P = 0.001) while the other comparisons were insignificant. In the medium compartment and anode compartment, the pH obtained did not have a statistically significant difference (P = 0.437 and P = 0.454, respectively).

$$2H_2O \rightarrow 4e^- + 4H^+_{(aq)} + O_{2(g)} \quad (2)$$

$$4H_2O + 4e^- \rightarrow 2H_{2(g)} + 4OH^-_{(aq)} \quad (3)$$

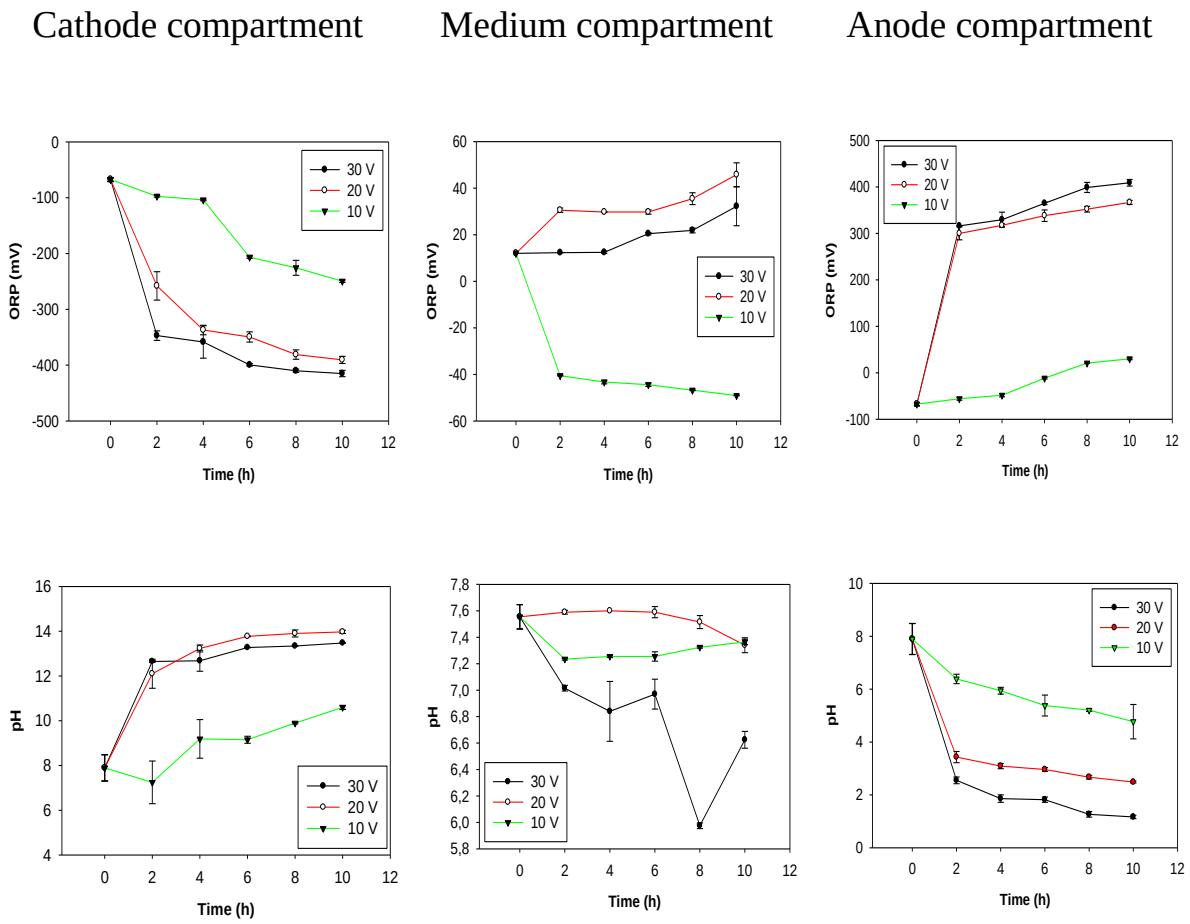

Fig. 5. Time course of ORP and pH in the three compartments of the electrokinetic system at the voltages of 30 V, 20 V and 10 V. Results represent the mean of three experiments, and errors bars represent the standard deviation.

3.5 Extraction and recovery of biosurfactants

The recovery of biosurfactants using the electrokinetic system was evaluated on the hypothesis that if the biosurfactants have a charge, then they could migrate to either of the oppositely charged electrodes (electrode compartments) and would be retained their free from the broth, cells and any other impurities which would remain in the medium compartment. The double diffusion method used to determine the ionic charge of the biosurfactant revealed that the biosurfactant was

anionic in nature since precipitation lines were observed between the biosurfactant and barium chloride. This is similar to previous reports in which a biosurfactant produced by *Pseudomonas aeruginosa* was revealed to be a rhamnolipid after it exhibited identical characteristics [21].

After biosurfactant production in the Erlenmeyer flasks under optimum conditions, biosurfactant broth was introduced into the electrokinetic reactor for biosurfactant extraction, recovery, and purification. After 4 h of operation, the turbidity of the anolyte kept increasing for the duration of the experiment when 30 V was applied. Under the application of 20 V, the turbidity of the anolyte started increasing after 6 h, while the same was only observed after 8 h when 10 V was applied. The extraction process is, therefore, dependent on the voltage applied to facilitate the electromigration of colloidal biosurfactants. The increase in the turbidity of the anolyte was followed by the continuous accumulation of aggregated greenish colloids on the floor of the anode compartments. The pH in the anode compartments was also continuously decreasing while increasing at the cathode from an initial pH of 7.895 ± 0.42 in all experiments. After 10 h the pH at the anode had reached 1.165 ± 0.05, 2.485 ± 0.03 and 4.77 ± 0.46 for 30 V, 20 V and 10 V, respectively. Simultaneously, the electrolyte (anolyte) reduced in the anode compartments with a proportional increase in the cathode compartments because of EOF. The reduction of the anolyte in the anode compartment allowed the biosurfactant extract to be recovered, air-dried and weighed after 10 h of the electrokinetic extraction process. In experiments where EOF was low, such as in

the 10 V and 20 V experiments, the water content (anolyte) was still predominant. The biosurfactants were further recovered from the anolyte by eliminating the supernatant by centrifugation or evaporation of the anolyte in an oven. The quantification of the biosurfactants recovered at every voltage is shown in **Fig. 6a**. The highest voltage of 30 V facilitated the highest extraction and recovery of biosurfactants at 69.33 ± 3.67 %; this was followed by 20 V with 9.63 ± 0.4 % and 10 V with 4.98 ± 0.46 %. At 20 V, the recovery was almost as twice (1.94) as that obtained at 10 V, but the increment of the voltage from 20 V to 30 V increased the recovery by 7-folds. This shows that the highest voltage possible is required to achieve the most efficient extraction of biosurfactants. The values of biosurfactant recovery obtained showed a statistically significant difference when 30 V and 20 V were compared ($P = 0.001$), while the other comparisons were insignificant since the differences were not high enough.

When the potentially recovered biosurfactant from the electrokinetic system was evaluated using SEM and EDX it was revealed that the extract was made up of spherical aggregates with particle sizes of approximately 100 nm. Rhamnolipids are generally weak acids that can undergo coalescence due to the presence of carboxylic acid moieties in their molecules [36, 37]. The anionic nature of a rhamnolipid biosurfactant is due to its carboxyl group which is strongly affected by the ionic strength of the solution/electrolyte [37]. In the absence of an electrolyte, the carboxyl groups dissociate to form carboxylate

groups. In contrast, in the presence of an electrolyte, the carboxylate groups are shielded by a diffuse layer of counterions which leads to the increase in the ionic strength of the medium [37]. When the concentration of rhamnolipids reaches the critical micelle concentration, the micelles aggregate depending on the pH, the concentration of the biosurfactant and the electrolyte [21]. This explains why there was aggregation of biosurfactant colloids after they electrophoretically moved into the anode compartment where the conditions were highly acidic at all voltages. The higher increase in the turbidity of the anolyte when 30 V was applied compared to other voltages resulted from the high extraction and aggregation of biosurfactant colloids due to the intensity of the electric field. The formation of spherical micelles after aggregation of the colloidal biosurfactant is similar to reports made in previous studies where spherical and rod-shaped micelles were formed [37, 38]. The growth of the micelles is highly dependent on the repulsive forces between similar charges since aggregation only happens when the repulsive forces are lowered [39]. In an electrokinetic system where EOF of the electrolyte is abundant, hydrational, steric surface forces, electrostatic, and van der Waals forces are responsible for the electrostatic stabilisation of colloidal biosurfactants [37]. The aggregation of the biosurfactants is followed by the formation of hard spherical models, as seen in **Fig. 6b**. Helvacı et al. [37] claim that hard sphere models exhibit a configuration of folded rhamnosyl groups under aggregated hydrophobic tails where the hydroxyl groups take up lateral positions to form a compact monomolecular layer

of rhamnolipid molecules. The formation of a compact monomolecular layer is a result of hydrogen bridges formed between moieties of rhamnosyl groups in the monolayer subphase enhanced by lateral positions of the hydroxyl groups [37].

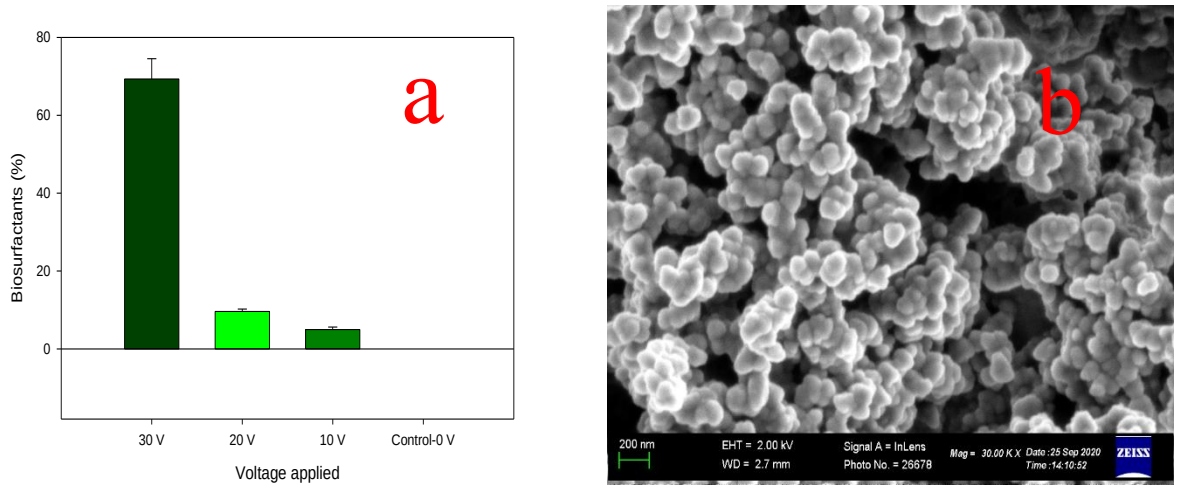

Fig. 6. Bar chart showing the recovery rate of the biosurfactant in the electrokinetic system at 30 V, 20 V and 10 V (**Fig. 6a**, results are a representation of the mean of three experiments, and error bars represent the standard deviation) and the SEM micrograph showing the morphology and size of the biosurfactant recovered in the electrokinetic system (**Fig. 6 b**).

3.6 Purity of the biosurfactant recovered

3.6.1 Fourier transform infrared spectroscopy characterisation of biosurfactants.

The purity of the biosurfactants recovered was evaluated by comparing the functional groups of the biosurfactant recovered using acid precipitation (Acid_Bio) and that recovered using the electrokinetic system at 30 V, 20 V and 10 V (EKS_Bio_30 V, EKS_Bio_20 V, EKS_Bio_10 V) as seen in **Fig. 7**. The

analysis of the spectra revealed that the functional groups of the extract obtained by acid precipitation were similar to the functional groups of the extract recovered from the electrokinetic system. The chemical functional groups of the biosurfactants obtained between 4000 cm^{-1} and 400 cm^{-1} for both acid precipitation and that recovered using the electrokinetic system revealed that the extract recovered by both methods was a glycolipid which is rhamnolipid in nature [18, 25]. The weak and broad absorption bands at 3176 cm^{-1} for Acid_Bio, 3062 cm^{-1} for EKS_Bio_30 V, 3180 cm^{-1} for EKS_Bio_20 V and 3179 cm^{-1} for EKS_Bio_10 V represent -OH stretching, the aromatic overtones between 2000 cm^{-1} and 1650 cm^{-1} in all the spectra represent the C-H bending, the weak strong absorption bands at 1648 cm^{-1} for Acid_Bio, 1650 cm^{-1} for EKS_Bio_30 V, 1651 cm^{-1} for EKS_Bio_20 V and 1648 cm^{-1} for EKS_Bio_10 V represent the C=O stretching, medium absorption bands between 1465 cm^{-1} and 1450 cm^{-1} in all spectra represent C-H bending, C-O-C stretching is represented by strong and broad bands at 1010 cm^{-1} for EKS_Bio_30 V and EKS_Bio_20 V, 1020 cm^{-1} for EKS_Bio_10 V and 1061 cm^{-1} for Acid_Bio, C-H bending is further revealed by strong absorption bands at 863 cm^{-1} in spectra of all extracts recovered [18, 25].

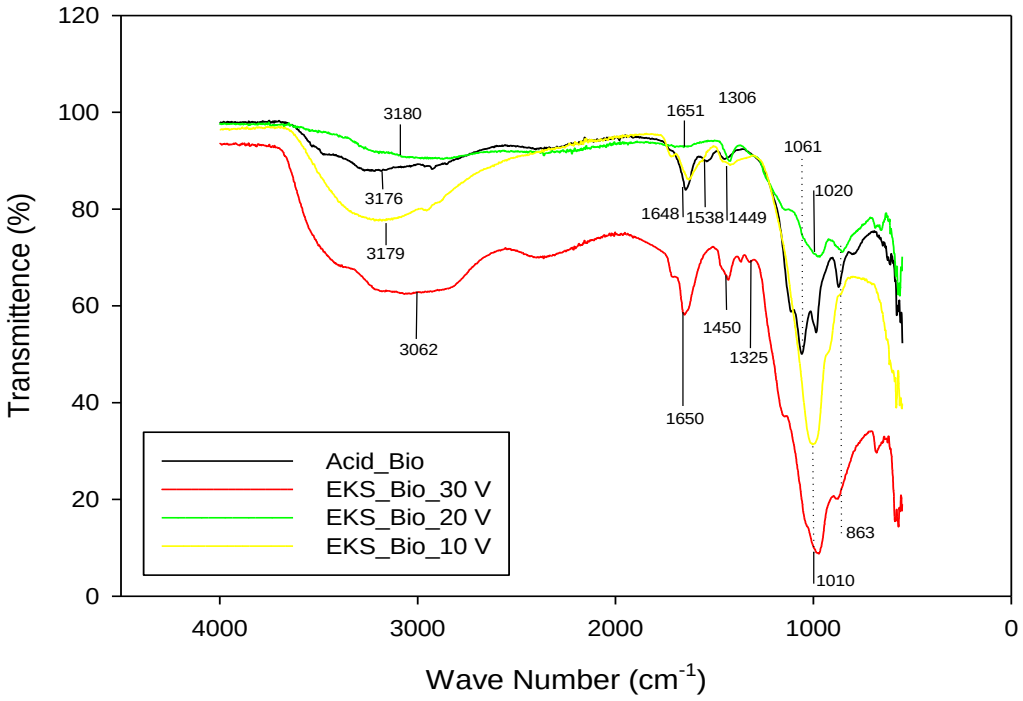

Fig. 7. Fourier-transform infrared spectra of the biosurfactants extracted by acid precipitation (Acid_Bio) and that extracted by the electrokinetic system at 30 V, 20 and 10 V (EKS_Bio_30 V, EKS_Bio_20 V and EKS_Bio_10 V.

3.6.2 Thin-layer chromatography analysis.

The biosurfactant recovered using acid precipitation (Acid_Bio), and that recovered using the electrokinetic system at different voltages (EKS_Bio_30 V, EKS_Bio_20 V and EKS_Bio_10 V) were separated on silica gel plates. The results revealed that all the biosurfactants were composed of the same mono-rhamnolipid congeners with an Rf of 0.75 and di-rhamnolipid congeners with an Rf of 0.33 as reported by other researchers [40, 41].

3.6.3 Identification of impurities by elemental composition analysis

The biosurfactant extracts recovered by the electrokinetic system had fewer impurities than the biosurfactant extracts recovered by acid precipitation (**Table 2**). The dominant impurities in the biosurfactant recovered by the electrokinetic system were mainly silicon, phosphorus and iron, whereas the biosurfactant recovered by acid precipitation mainly had impurities of sodium, potassium, sulphur, silicon, and phosphorus, with phosphorus as the most dominant impurity. The difference in the composition is the reason for the differences in the colours of the biosurfactant extracts, with the one recovered by acid precipitation taking up a brownish colour and the one recovered by the electrokinetic system taking up a greenish colour (**Fig. 8a**). The biosurfactant extract obtained by acid precipitation was 71.09% pure as compared to biosurfactant extract obtained by the electrokinetic system that had 72.88% purity

Table 2. Elemental composition of the biosurfactant recovered by acid precipitation and electrokinetic extraction

	Acid Precipitation	Electrokinetic Recovery
Element	Wt%	Wt%
C	27.26	31.73
O	43.83	41.15
Na	6.96	—
Mg	0.30	—
Al	0.30	—
Si	3.35	2.35
P	10.43	9.40
S	1.84	—

Cl	0.15	—
K	4.27	0.62
Ca	0.73	—
W	0.56	—
Fe	—	14.75
Total:	100.00	100.00

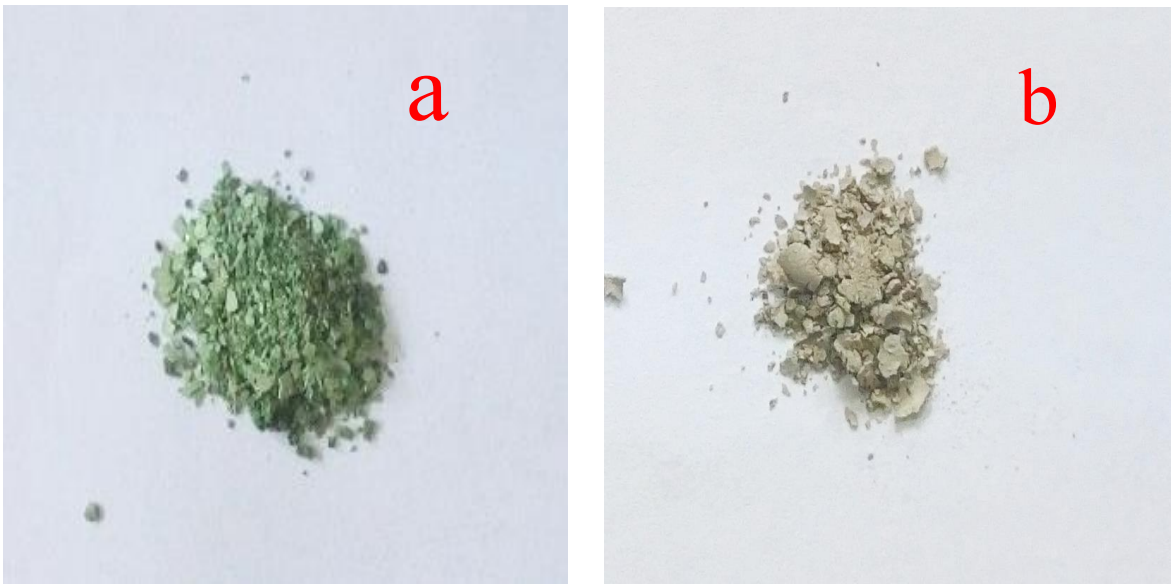

Fig. 8. The samples of the biosurfactant recovered by the electrokinetic system (Fig. 8a) and that recovered by acid precipitation (Fig.8b).

The comparison of different rhamnolipid extraction methods used by Invally et al. [7] were compared to the electrokinetic extraction method used in this study (**Table 3**). The methods adopted for comparisons with electrokinetic extraction (EK) were acid precipitation (AP), solvent extraction (SE), reverse extraction (RE), alcohol precipitation (OP), and calcium precipitation (CP). The comparisons show that the electrokinetic method had better recovery outcomes than acid precipitation-solvent extraction and acid precipitation-solvent extraction-reverse extraction, much as the biosurfactant concentration in the culture broth was only 10.2 ± 2.4 g/L. However, the purity of the biosurfactant

was slightly lower than all the other methods because a combination of more than one method was used to improve the purity of the biosurfactant recovered.

Table 3. Comparisons of biosurfactant extraction methods

No.	Extraction method	Biosurfactant concentration in broth (g/L)	Recovery (%)	Purity (%)	Reference
1.	AP + SE	49.7 ± 6.8	65.5 ± 9.9	84.1 ± 7.4	[7]
2.	AP+ SE + RE	49.7 ± 6.8	64.3 ± 10.3	Not analysed	[7]
3.	OP + AP	49.7 ± 6.8	77.8 ± 11.8	86.9 ± 13.7	[7]
4.	OP + AP + CA	49.7 ± 6.8	72.0 ± 10.9	95.4 ± 0.5	[7]
5.	EK	10.2 ± 2.4 g/L	69.33 ± 3.67	72.88 ± 6.34	In this study

3.7 Energy expenditure of the electrokinetic extraction process

The energy budget was determined according to the equation below (Eq. (**4**)) where V_S is the volume of the medium (biosurfactant broth), I is the electric current in the system and V is the potential difference between the electrodes. E_u is calculated as kWh m^{-3} [42]. As seen in **Fig. 9**, the highest energy was observed for 30 V at 783.38 ± 16.13 $kWhm^{-3}$, followed by 20 V at 304.25 ± 5.25 $kWhm^{-3}$ and 10 V at 54.63 ± 0.38 $kWhm^{-3}$. Energy expenditure is a function of voltage

and time; therefore, the higher the voltage, the higher the energy budget if the time is constant. The rate of biosurfactant extraction depends on the voltage applied; therefore, a high voltage is meant to offer higher efficiency in terms of biosurfactant extraction and recovery. A lower voltage such as 10 V would likely provide a lower energy budget, but if the same amount of extraction as that of 30 V is to be achieved, it would require a longer operational time. This means that its most likely that the energy budget would ultimately be as high as that of 30 V. Comparing the voltages applied, the energy budget per unit of biosurfactant recovered was 11 $kWhm^{-3}$ for 30 V, 31 $kWhm^{-3}$ for 20 V and 10.99 $kWhm^{-3}$ for 10 V. It was therefore cheaper to extract the biosurfactant at a higher voltage of 30 V than a lower voltage of 20 V.

$$E_u = \frac{1}{V_S} \int VIdt \tag{4}$$

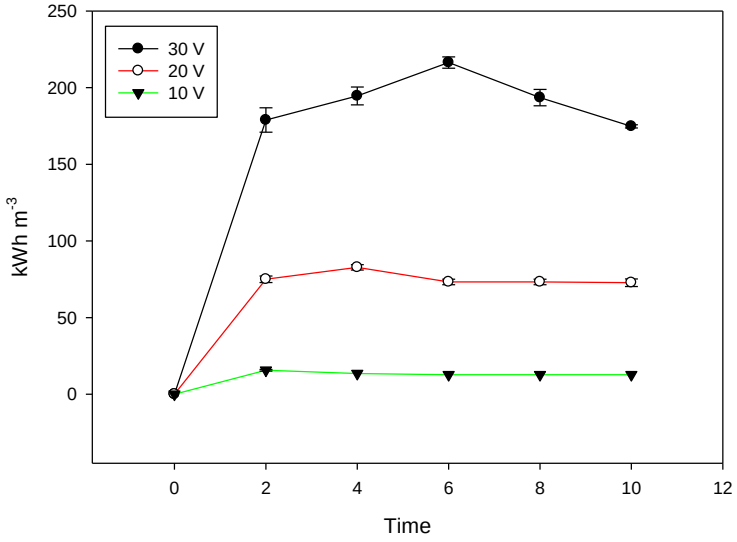

Fig. 9. Time course of the energy expenditures during extraction of the biosurfactant in the electrokinetic system at 30 V, 20 V and 10 V. Results represent the mean of three experiments, and errors bars represent the standard deviation.

3.8 Cost estimations of electrokinetic extraction and acid precipitation of biosurfactants

In the estimations of costs for the electrokinetic extraction of biosurfactants presented in **Table 4**, the cost of energy, the cost of reactor construction, the cost of electrodes, variable costs and fixed costs were considered as adapted from previous studies (Gidudu and Chirwa, 2020). In estimating the costs, the energy expenditure of the extraction process using 30V was used since it was the most efficient. The total cost for the electrokinetic extraction of biosurfactants from 800 mL (0.0008m^3) of broth at a bench scale was determined as US$1354.525. In the cost estimations for the acid precipitation method, the equipment and the

chemicals used in the process were majorly considered since the process does not require intensive technical setups but requires several types of equipment. The total cost of processing 800 mL of broth to recover the biosurfactant by acid precipitation was US$33619.66 (**Table 4**). The total costs for the recovery of the biosurfactant from 800 mL of broth may require 25 folds more capital using acid precipitation than electrokinetic extraction. These costs may, however, extensively change with an increase in the volume of culture broth processed. The cost of acid precipitation may reduce with an increase in the volume of broth because of the once-off cost of equipment that may be required. This would be different for the electrokinetic extraction process, whose cost may increase with the increase in volume due to the high dependence on energy.

Table 4. Cost estimations for the recovery of the biosurfactant using electrokinetic extraction and acid precipitation

Electrokinetic extraction					
No.	Item	Unit cost in US$	Quantity	Total cost in US$	Reference
1.	Cost of electrodes per unit height (reusable)	5/m	0.1m	0.5	Gidudu and Chirwa [22]
2.	Cost of energy	0.04/kWh	11kWhm^{-3} for 30V	$11 \times 0.04 \times 0.0008 = 0.000352$	Gidudu and Chirwa [22]
3.	Cost of reactor fabrication	5/m	1.14m (Reactor perimeter)	$1.14 \times 5 = 5.7$	Gidudu and Chirwa [22]

4.	Variable cost (Labour)	25/man*h	1-man crew for 10h	$25 \times 10 = 250$	Gidudu and Chirwa [22]
5.	Variable cost including insurance	0.001/m^3/h	0.0008m^3 for 10h	$0.001 \times 0.0008 \times 10 = 0.000008$	Gidudu and Chirwa [22]
6.	Fixed costs	25/m^3	0.001m^3	$25 \times 0.001 = 0.025$	Gidudu and Chirwa [22]
7.	Evaporator, Power supply and	1100	1	750	N/A
8.	Miscellaneous	354	1	354	N/A
	Total cost			1354.525	

Acid Precipitation

No.	Item	Unit cost in US$	Quantity	Total cost in US$	Reference
1.	Centrifuge separator equipment	8000	1	8000	N/A
2.	Incubator	25000	1	25000	N/A
3.	Filters	14	1	14	N/A
4.	Hydrochloric acid	20/L	0.04L	$20 \times 0.04 = 0.8$	N/A
5.	Methanol	2/L	0.04L	$2 \times 0.04 = 0.08$	N/A
6.	Chloroform	19/L	0.04L	$19 \times 0.04 = 0.76$	N/A
7.	Evaporator	354	1	354	N/A
8.	Variable cost (Labour)	25/man*h	1-man crew for 10h	$25 \times 10 = 250$	Gidudu and Chirwa [22]
9.	Variable cost including insurance	0.001/m^3/h	0.0008m^3 for 10h	$0.001 \times 0.0008 \times 10 = 0.000008$	Gidudu and Chirwa [22]

10.	Fixed costs	25/m^3	0.0008m^3	$25 \times 0.0008 = 0.02$	Gidudu and Chirwa [22]
11.	Miscellaneous	354	1	354	N/A
	Total cost			33619.66	

4. Conclusion

Biosurfactants can effectively be extracted and recovered using the electrokinetic system. The rate of extraction is dependent on the voltage/current applied since the highest voltage of 30 V had the highest recovery of 69.32 ± 3.6715 %. In comparison, the lowest voltage of 10 V only achieved a recovery of 4.98 ± 0.4585 %. The biosurfactant extract recovered using the electrokinetic system had fewer impurities than the biosurfactant extract recovered using acid precipitation. The energy budget increases with the increase in voltage applied, but the highest voltage is cheaper than the lowest voltage in terms of per unit mass of the biosurfactant extracted and recovered. The electrokinetic system can therefore be used as a sustainable alternative for biosurfactant extraction and recovery. Sustainable sources of energy such as solar energy can be used to reduce the carbon footprint of the process. More research could be required to further analyse the extract and model the extraction process through advanced kinetic studies.

CRediT authorship contribution statement

Brian Gidudu: Conceptualisation, investigation, validation, writing draft, software, formal analysis, review, and editing**. Evans M.N Chirwa:** Supervision, methodology, review and editing, resources, administration**.**

Declaration of competing interest

The authors declare that they have no known competing financial interests or personal relationships that could have appeared to influence the work reported in this paper.

Acknowledgment

This research was fully funded by the University of Pretoria and National Research Foundation (NRF_DST). It is indeed in the authors at most interest to appreciate the financial support offered in that regard.

Nomenclature

FTIR	Fourier transform infrared spectroscopy
TLC	Thin layer chromatography
Rf	Retardation factor
ORP	Oxidation reduction potential
EOF	Electroosmotic flow
UPLC-MS	Ultra-performance liquid chromatography-mass spectrometry
SEM	Scanning electron microscopy
rpm	revolutions per minute
EDX	Energy dispersive x-ray
US$	United States Dollar
D	dielectric constant
ε_0	vacuum permittivity
l	fluid viscosity

References

[1] S.J. Varjani, V.N. Upasani, Critical review on biosurfactant analysis, purification and characterisation using rhamnolipid as a model biosurfactant, Bioresour. Technol. 232 (2017) 389-397.

[2] T.A. Ostendorf, I.A. Silva, A. Converti, L.A. Sarubbo, Production and formulation of a new low-cost biosurfactant to remediate oil-contaminated seawater, J. Biotechnol. 295 (2019) 71-79.

[3] A.A. Jimoh, J. Lin, Biosurfactant: A new frontier for greener technology and environmental sustainability, Ecotoxicol. Environ. Saf. 184 (2019) 109607.

[4] R.M.S. Cameotra, An update on the use of unconventional substrates for biosurfactant production and their new applications, Appl. Microbiol. Biotechnol. 58 (2002) 428-434.

[5] K. Sałek, S.R. Euston, Sustainable microbial biosurfactants and bioemulsifiers for commercial exploitation, Process Biochem. 85 (2019) 143-155.

[6] M. Heyd, A. Kohnert, T.H. Tan, M. Nusser, F. Kirschhöfer, G. Brenner-Weiss, M. Franzreb, S. Berensmeier, Development and trends of biosurfactant analysis and purification using rhamnolipids as an example, Anal. Bioanal. Chem. 391 (2008) 1579-1590.

[7] K. Invally, A. Sancheti, L.-K. Ju, A new approach for downstream purification of rhamnolipid biosurfactants, Food Bioprod. Process 114 (2019) 122-131.

[8] S. Mukherjee, P. Das, R. Sen, Towards commercial production of microbial surfactants, Trends Biotechnol. 24 (2006) 509-515.

[9] B. Barman, D. Kumar, P.P. Gopmandal, H. Ohshima, Electrokinetic ion transport and fluid flow in a pH-regulated polymer-grafted nanochannel filled with power-law fluid, Soft Matter 16 (2020) 6862-6874.

[10] T. Muddemann, D. Haupt, M. Sievers, U. Kunz, Electrochemical reactors for wastewater treatment, ChemBioEng Rev. 91 (2019) 769-785

[11] E. Mena, J. Villaseñor, M.A. Rodrigo, P. Cañizares, Electrokinetic remediation of soil polluted with insoluble organics using biological permeable reactive barriers: Effect of periodic polarity reversal and voltage gradient, Chem. Eng. J. 299 (2016) 30-36.

[12] A. Poddar, D. Maity, A. Bandopadhyay, S. Chakraborty, Electrokinetics in polyelectrolyte grafted nanofluidic channels modulated by the ion partitioning effect, Soft Matter 12 (2016) 5968-5978.

[13] K. Popov, I. Glazkova, V. Yachmenev, A. Nikolayev, Electrokinetic remediation of concrete: effect of chelating agents, Environ. Pollut. 153 (2008) 22-28.

[14] R.J. Fritsch, I. Krause, Electrophoresis, in: B. Caballero (Ed.) Encyclopedia of Food Sciences and Nutrition (Second Edition), Academic Press, Oxford, 2003, pp. 2055-2062.

[15] M.O. Boulakradeche, D.E. Akretche, C. Cameselle, N. Hamidi, Enhanced Electrokinetic Remediation of Hydrophobic Organics Contaminated Soils by the Combination of Non-Ionic and Ionic Surfactants, Electrochim. Acta 174 (2015) 1057-1066.

[16] R.S. Makkar, K.J. Rockne, Comparison of synthetic surfactants and biosurfactants in enhancing biodegradation of polycyclic aromatic hydrocarbons, Environ. Toxicol. Chem. 22 (2003) 2280–2292.

[17] J. Radjenovic, D.L. Sedlak, Challenges and opportunities for electrochemical processes as next-generation technologies for the treatment of contaminated water, Environ. Sci. Technol. 49 (2015) 11292-11302.

[18] B. Gidudu, E.M.N. Chirwa, Application of biosurfactants and pulsating electrode configurations as potential enhancers for electrokinetic remediation of petrochemical contaminated soil, Sustainability 12 (2020).

[19] K. Trummler, F. Effenberger, C. Syldatk, An integrated microbial/enzymatic process for production of rhamnolipids and L-(+)-rhamnose from rapeseed oil with Pseudomonas sp. DSM 2874, Eur. J. Lipid Sci. Technol. 105 (2003) 563–571.

[20] P. Noparat, S. Maneerat, A. Saimmai, Utilisation of palm oil decanter cake as a novel substrate for biosurfactant production from a new and promising strain of Ochrobactrum anthropi 2/3, World J. Microbiol. Biotechnol. 30 (2014) 865-877.

[21] I.J.B. Durvala, A.H.R. Mendonça, I.V. Rochad, J.M. Lunab, R.D. Rufinob, A. Convertie, L.A. Sarubbob, Production, characterisation, evaluation and toxicity assessment of a Bacillus cereus UCP 1615 biosurfactant for marine oil spills bioremediation, Mar. Pollut. Bull. 157 (2020) 111357.

[22] B. Gidudu, E.M.N. Chirwa, The combined application of a high voltage, low electrode spacing, and biosurfactants enhances the bio-electrokinetic remediation of petroleum contaminated soil, J. Clean. Prod. 276 (2020) 122745.

[23] S.M. Dastgheib, M.A. Amoozegar, E. Elahi, S. Asad, I.M. Banat, Bioemulsifier production by a halothermophilic Bacillus strain with potential applications in microbially enhanced oil recovery, Biotechnol. Lett. 30 (2008) 263-270.

[24] G.S. Shreve, R. Makula, Characterisation of a New Rhamnolipid Biosurfactant Complex from Pseudomonas Isolate DYNA270, Biomolecules 9 (2019) 885.

[25] A. Fadhile Almansoory, H. Abu Hasan, M. Idris, S.R. Sheikh Abdullah, N. Anuar, E.M. Musa Tibin, Biosurfactant production by the hydrocarbon-degrading bacteria (HDB) Serratia marcescens : Optimisation using central composite design (CCD), J. Ind. Eng. Chem. 47 (2017) 272-280.

[26] B. Gidudu, E.M.N. Chirwa, Production of a bacterial biosurfactant in an electrochemical environment as a prelude for in situ biosurfactant enhanced bio-electrokinetic remediation, Process Saf. Environ. 148 (2021) 676-685.

[27] C. Cameselle, S. Gouveia, D. Eddine, B. Belhadj, Advances in electrokinetic remediation for the removal of organic contaminants in soils, in: organic pollutants-monitoring, risk and treatment, 2013. e-book. https://doi.org/10.5772/54334. (Accessed 20 February 2021).

[28] W. Liu, Y. Tao, Z. Ge, J. Zhou, R. Xu, Y. Ren, Pumping of electrolyte with mobile liquid metal droplets driven by continuous electrowetting: A full-scaled simulation study considering surface-coupled electrocapillary two-phase flow, Electrophoresis 42 (2020) 950-966.

[29] E. Li, Y. Pan, C. Wang, C. Liu, C. Shen, C. Pan, X. Liu, Multifunctional and superhydrophobic cellulose composite paper for electromagnetic shielding, hydraulic triboelectric nanogenerator and Joule heating applications, Chem. Eng. J. 420 (2021) 129864.

[30] L. Yang, G. Nakhla, A. Bassi, Electrokinetic dewatering of oily sludges, J. Hazard. Mater. 125 (2005) 130-140.

[31] E. Mena Ramirez, J. Villasenor Camacho, M.A. Rodrigo, P. Canizares, Combination of bioremediation and electrokinetics for the in-situ treatment of diesel polluted soil: A comparison of strategies, Sci. Total Environ. 533 (2015) 307-316.

[32] S. Xu, S. Guo, B. Wu, F. Li, T. Li, An assessment of the effectiveness and impact of electrokinetic remediation of pyrene contaminated soil, J. Environ. Sci. 26 (2014) 2290-2297.

[33] V.R. Ouhadi, R.N. Yong, N. Shariatmadari, S. Saeidijam, A.R. Goodarzi, M. Safari-Zanjani, Impact of carbonate on the efficiency of heavy metal removal from kaolinite soil by the electrokinetic soil remediation method, J. Hazard. Mater. 173 (2010) 87-94.

[34] M.G. Cikalo, K.D. Bartle, P. Myers, Influence of the electrical double-layer on electroosmotic flow in capillary electrochromatography, J. Chromatogr. A 836 (1999) 35-51.

[35] E.K. Jeon, J.M. Jung, W.S. Kim, S.H. Ko, K. Baek, In situ electrokinetic remediation of As-, Cu-, and Pb-contaminated paddy soil using hexagonal electrode configuration: a full scale study, Environ. Sci. Pollut. Res. Int. 22 (2015) 711-720.

[36] L.M. Wu, L. Lai, Q. Lu, P. Mei, Y.Q. Wang, L. Cheng, Y. Liu, Comparative studies on the surface/interface properties and aggregation behavior of mono-rhamnolipid and di-rhamnolipid, Colloids Surf. B Biointerfaces, 181 (2019) 593-601.

[37] S.S. Helvacı, S. Peker, G. Özdemir, Effect of electrolytes on the surface behavior of rhamnolipids R1 and R2, Colloids Surf. B: Biointerfaces 35 (2004) 225-233.

[38] H. Zhong, Y. Jiang, G. Zeng, Z. Liu, L. Liu, Y. Liu, X. Yang, M. Lai, Y. He, Effect of low-concentration rhamnolipid on adsorption of Pseudomonas aeruginosaATCC 9027 on hydrophilic and hydrophobic surfaces, J. Hazard. Mater. 285 (2015) 383-388.

[39] S. Miyagishi, N. Takeuchi, T. Asakawa, M. Inoh, Micellar growth of N-dodecanoyl-alaninates with different counterions and its quantitative relation with some fa, Colloids Surf. A Physicochem. Eng. Asp. 197 (2002) 125-132.

[40] P. Das, X.-P. Yang, L.Z. Ma, Analysis of biosurfactants from industrially viable Pseudomonas strain isolated from crude oil suggests how rhamnolipids congeners affect emulsification property and antimicrobial activity, Front. microbiol. 5 (2014) 696.

[41] M. Aghajani, A. Rahimpour, H. Amani, M.J. Taherzadeh, Rhamnolipid as new bio-agent for cleaning of ultrafiltration membrane fouled by whey, Eng. Life Sci. 18 (2018) 272–280.

[42] K.R. Reddy, R.E. Saichek, Enhanced electrokinetic removal of phenanthrene from clay soil by periodic electric potential application, J. Environ. Sci. Health A 39 (2004) 1189-1212.

Captions of schematic views

Scheme 1. Schematic view of the electrokinetic system setup

Captions of Figures

Fig. 1. Mass-Charge spectrum of the biosurfactant obtained by liquid chromatography tandem mass spectrometry

Fig. 2. Time course of current in the electrokinetic system at different voltages of 30 V, 20 V and 10 V.

Fig. 3. Time course of conductivity and temperature in the three compartments of the electrokinetic system as a function of different voltages applied. Results are a representation of the mean of three experiments, and errors bars represent the standard deviation.

Fig. 4. Electroosmotic flow in the electrokinetic system as a function of different voltages applied. Results are a representation of the mean of three experiments, and errors bars represent the standard deviation.

Fig. 5. Time course of ORP and pH in the three compartments of the electrokinetic system at the voltages of 30 V, 20 V and 10 V. Results represent the mean of three experiments, and errors bars represent the standard deviation.

Fig. 6. Bar chart showing the recovery rate of the biosurfactant in the electrokinetic system at 30 V, 20 V and 10 V (**Fig. 6a**, results are a representation of the mean of three experiments, and error bars represent the standard deviation) and the SEM micrograph showing the morphology and size of the biosurfactant recovered in the electrokinetic system (**Fig. 6 b**).

Fig. 7. Fourier-transform infrared spectra of the biosurfactants extracted by acid precipitation (Acid_Bio) and that extracted by the electrokinetic system at 30 V, 20 and 10 V (EKS_Bio_30 V, EKS_Bio_20 V and EKS_Bio_10 V).

Fig. 8. The samples of the biosurfactant recovered by the electrokinetic system (Fig. 8a) and that recovered by acid precipitation (Fig.8b).

Fig. 9. Time course of the energy expenditures during extraction of the biosurfactant in the electrokinetic system at 30 V, 20 V and 10 V. Results represent the mean of three experiments, and errors bars represent the standard deviation.

Captions of Tables

Table 1. Components of the rhamnolipid biosurfactant

Table 2. Elemental composition of the biosurfactant recovered by acid precipitation and electrokinetic extraction

Table 3. Comparisons of biosurfactant extraction methods

Table 4. Cost estimations of the biosurfactant recovery process using electrokinetic extraction and acid precipitation